InfoTech Spectrum: Iraqi Journal of Data Science (IJDS)
ISSN: 3007-5467, Vol 2(No.1), 26-36 (2025)
DOI: https://doi.org/10.51173/ijds.v1i1.13
https://ijds.mtu.edu.iq

MEDICAL IMAGE COMPRESSION UTILIZING THE SERIAL DIFFERENCES AND CODING TECHNIQUES

Ghalib Ahmed Salman [1*], Ahmed Ghalib Ahmed [2], Hareer Moaiad Hussen [3]

[1,2,3] *Electrical Engineering Technical College, Middle Technical University, Baghdad, Iraq*

* *Corresponding author E-mail: dr.ghalib@mtu.edu.iq (Ghalib Ahmed Salman)*

RESEARCH ARTICLE

ARTICLE INFORMATION

SUBMISSION HISTORY:

Received: 26 July 2024
Revised: 4 January 2025
Accepted: 23 January 2025
Published: 30 January 2025

KEYWORDS:

Serial Medical Images;
Huffman Coding;
Run Length Encoding;
near-Lossless compression;
image compression.

ABSTRACT

Different medical devices for imaging used by centers and clinics produce an increasing number of sequential medical images. Different imaging techniques such as Computed Tomography (CT), Magnetic Resonance Imaging (MRI) and Fluoroscopy produce a set of series for the same patient. Within these images, most of the image parts are fixed against noticeable changes in the remaining part. This consumes non-ignorable storage space. This paper proposes a near-lossless compression technique that considers the fixed image parts to focus on changing parts for a higher compression ratio. In some applications, lossless compression techniques are highly preferable against preferring lossy techniques in some applications. In other applications, near-lossless compression techniques are preferable to lossless and lossy compression techniques, where lossy ones may lose significant details, and the lossless ones produce less compression ratios than near-lossless ones. Previous works dealt with Fluoroscopy images as individual images or using video compression techniques. This work tends to handle the whole series of images as an integrated object. This paper considers subtracting successive images to detect ROI areas producing zero overall values over similar areas and non-zero ones within ROI ones. The double coding technique and near-lossless concept of compression increase the compression ratio. Conducted experiments showed encouraging results benchmarking the other published works in medical image compression.

1. INTRODUCTION

Recently, many serial medical images were generated, transmitted and saved. A considerable number researches were conducted to develop compression techniques for medical images [1]. Due to the originality of compressed information, compression approaches are divided into Lossless, Near-Lossless, and Lossy approaches [2]. Initially, a lossless compression approach is necessary to handle medical images due to the sensitivity of contained information, where the Compression Ratio (CR) is significantly lower than lossy and near-lossless approaches [3]. Conversely, some loss levels are acceptable, and the decompressed images are medically accepted, whereas the Peak Signal Noise Ratio (PSNR) is used to evaluate the decompressed images [4]. Depending on the PSNR value, the decompressed image is decided to represent the original image or not [5]. By preserving considerable PSNR value, near-lossless compression produces higher CR than lossless compression without losing image details, as in lossy compression. One of the most effective compression methods is the coding techniques such as Huffman, arithmetic, Run Length Encoding (RLE), and others. In previous literature, combining more than one encoding technique yielded better results, and due to the specifics of the compressed data, applying one of them before the other may increase or decrease the CR [6]. Fluoroscopy images represent a set of images for the same patients, with fixed details in most image areas with small-area motion in specific parts. The main objectives of this paper are explained in three lines where the first is to minimize image information by focusing

DOI: https://doi.org/10.51173/ijds.v1i1.13

on the ROI area. The second one is to detect ROI areas by subtracting the successive images, which produces zero values overall in the image except for fluid-motion areas. The third one concerns increasing CR value using two approaches where the first approach is to apply the double-coding technique. The second approach ignores trivial values while ensuring the best PSNR to guarantee compressed-image quality.

This work considers applying near-lossless compression on Fluoroscopy images utilizing the subtraction between the successive Fluoroscopy images, where it considers keeping reference images and ignoring non-relative image parts. Besides, it considers applying more than one compression stage to increase the CR .The rest paper is organized as follows: Section 2 reviews the previously published literature in the field, and Section 3 summarizes the specifications of the studied Fluoroscopy images.

2. LITERATURE REVIEW

Although a considerable number of articles have been published in the Medical Image Compression field, recently, a few works of literature were published in the field of DICOM medical image compression due to different reasons [7]. Some of these reasons are related to image type, where several works adopted other types of medical images [2], [4]. Other reasons are related to the significant CR to be yielded, where many avoided working on Fluoroscopy images due to the huge size and the series of images for each patient [6, 7]. Gowda et al. [8] proposed a near-lossless compression method focusing on the Region of Interest (ROI) for medical images. The authors adopted the Vector Quantization combined with the standard Set Partitioning in Hierarchical Trees (SPIHT) coding techniques, where they extracted Digital Imaging & Communication in Medicine (DICOM)-image ROI depending on the standard Bounding Box technique. The SPIHT coding technique is then applied to encode ROI contents.

Conversely, non-ROI image sections were encoded using another encoding technique (Vector Quantization). The authors of another research proposed a compression method using a hybrid concept that improves the CR of medical images without degrading sensitive data. They implemented a threshold approach to segment image areas. Their ROI area was compressed using a lossless compression technique (Edge-Directed Prediction), where the areas were compressed by applying a lossy compression technique [9]. An image compression technique based on ROI area within the medical image was proposed, where they addressed frequent components of the studied image. The authors used fuzzy C-Means clustering to classify ROI and non-ROI areas. The ROI was compressed using a combination of Huffman, RLE encoding and Discrete Cosine Transform (DCT), while non-ROI areas were compressed using the Capsule Auto-Encoder technique [10].

3. PROPOSED METHODOLOGY

The primary concern of this paper depends on the fact that DVF consists of a reference image for the patient without any fluid motion besides the set of similar successive images. The majority of these successive images are the same with small-area changes.

3.1 Dicom Video Fluoroscopy (Dvf)

DVF is a technique of medical imaging that produces a series of sequential X-ray images to inspect the case of a single patient. Different procedures and inspections are used in its imaging technology, like catheterization, Barium Swallow, Percutaneous Nephrostomy (PCN), cardiac and others[11]. The patient drinks a fluid the clinical assistant gives, and fluid motion is captured along the Pharynx and Esophagus. DVF produces a reference image for each patient before starting the inspection fluid's motion, as in Figure 1-a. Then, the fluid starts moving through the patient's organs, as in Figures 1-b, c, d and e. Image parts from the outer black box then into a white circle, where

neither contains any medical information. They are the same for the whole series of images and can be replaced between any two images [11], [12]. Inside the white circle, a rectangle contains all the information about the patient's case, considered the ROI of DICOM images. Fig 1 shows the ROI rectangle highlighted by red boxes. A key difference between DICOM images and other types is that non-ROI areas (outside the inner rectangle) DO NOT contain any information. Ignoring non-ROI areas or replacing them between any two similar images has no degradation effects on the medical information contained in these images[13].

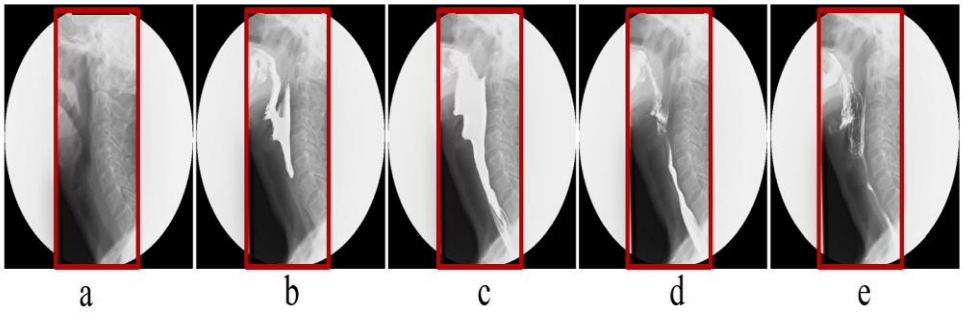

Figure 1: A series of DVF images for a single patient, where all medical information is contained in the inner rectangle highlighted by a red border.

3.2 Pre-Processing

The non-ROI (outer black box and the white circle) area is kept as a reference to compensate for the decompressed successive images and is compressed using lossy compression. All successive images are cropped into ROI areas, as in Fig 2, where they are compressed using more than one compression stage. Each ROI area is applied on the non-ROI border during decompression to retrieve the original DVF image.

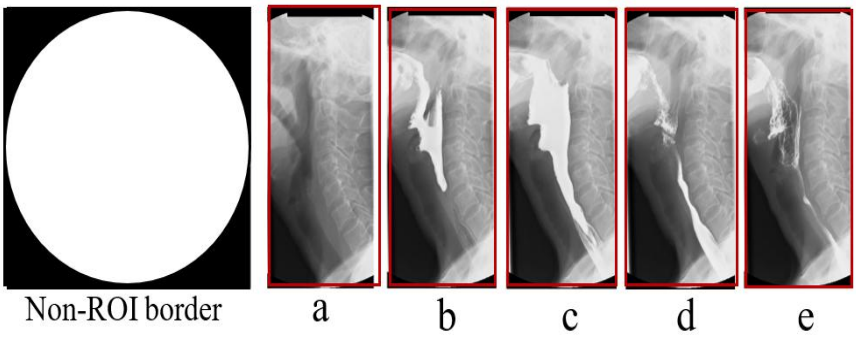

Figure 2: Illustrates preserving non-ROI reference and crop the other images into ROI area.

3.3 Compression Techniques:

This section discusses the adopted compression scheme in this work, which depends on major steps like Image separation into ROI & non-ROI areas, Compressing non-ROI using lossy compression, ROI detection by subtracting successive images, Ignoring trivial differences, and Double-Coding Compression for ROI area. The entire proposed compression scheme can be shown in Fig 3. In this figure, DICOM images are input, the ROI area is extracted, and the successive ones are subtracted. After ignoring trivial differences, RLE and Huffman's techniques are applied respectively, and then CR values are doubled. Non-ROI areas are compressed using lossy compression techniques and combined with the results of the Double-CR process to construct the compressed object.

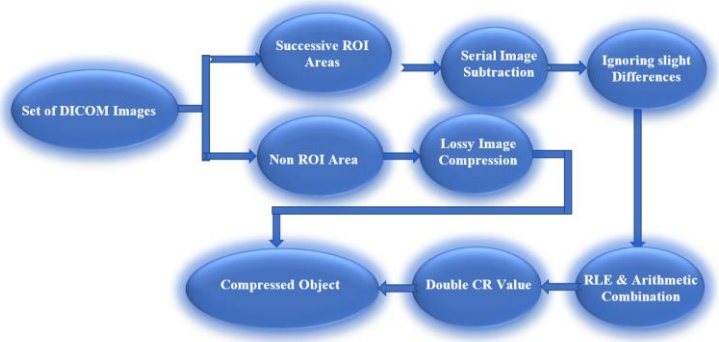

Figure 3: General diagram representing the proposed compression scheme for the DVF image

Instead of compressing each image, this methodology tends to compress the differences between the successive images. Due to the similar parts of the ROI area, most of the subtracted values will be zeros, and the non-zero values are concentrated within the fluid-motion area[14]. Fig 4 shows that most subtracted image values are converted into zero values (black areas), and non-zero values are noticed within fluid motion areas. Within the fluid-motion area, the values represent the differences between the corresponding values of the subtracted images rather than the original values.

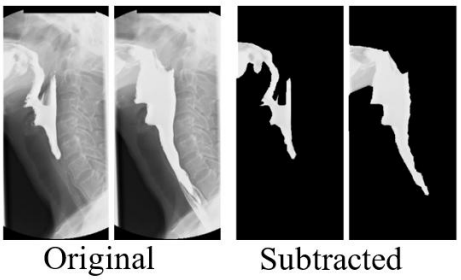

Figure 4: Image values converted to zeros in the subtracted area.

Finding image differences between sets of DICOM images has two major procedures. The first one is to find the difference between each image and the reference (first image in the series) considering motion difference from the original case of the patient. The second procedure is to find the difference between each two successive images considering the update difference in the patient test[15]. Each procedure has its advantages; the first provides detailed changes to the patient's original case. The second one measures the differences between too-close images, meaning maximum similarity and more zeros in different images providing higher CR. The last one can be justified by the correlation between DICOM images, which is measured using the Cross Correlation coefficient $r_{x,y}$ [16] using the following function:

$$r_{x,y} = \frac{\sum_{i=1}^{n}(x_i - \mu_x)(y_i - \mu_y)}{\sum_{i=1}^{n}(x_i - \mu_x)^2 \sum_{i=1}^{n}(y_i - \mu_y)^2} \qquad \dots (1)$$

Where x_i, y_i: are the pixel values from the subtracted images, μ_y, μ_y: are the average of pixel values in both images, n: is the number of pixels in each image.

The major concern of this step is to reach as high as possible CR for more efficient compression performance. This paper adopts two different compression techniques. Firstly, lossy compression for the non-ROI areas since the major concern is to increase CR regardless of contained (nonrelative) information. For this type of compression, this paper adopted one of the newest develops of the standard Joint Photographic Experts Group (JPEG) proposed by Husain et al. (2022) [17], where the authors used a fast fashion of Discrete Cosine Transform (DCT) to remove the majority of zeros keeping value position. In addition, they replaced the arithmetic coding technique

instead of the Huffman technique. Their technique was adopted in this paper due to the encouraging results for images containing a lot of zeros (as occurred in our non-ROI image), which were better than yielded results by standard fashion JPEG techniques by 1992 [18]. Lossless compression is mandatory for ROI areas to preserve sensitive information, yet an acceptable near-lossless compression significantly enhances the compression performance. This paper proposes a combination of compression steps as follows:

3.3.1 Coding Arrangement

This paper proposes combining RLE and Huffman coding to compress ROI-difference images. Firstly, Successive DICOM images share identical details in different parts of the serial images except the path of fluid motion. As a result, subtracting such images produces a lot of zero-value areas, where the RLE coding technique is an efficient compression technique for subtracted images. RLE combines lossless compression concepts and works on the same successive values [19]. Secondly, the result of RLE compression is represented by a series of values as in Fig 5, where these values do not record similar successive numbers to be compressed using RLE. Huffman coding technique can compress these values depending on their frequencies since it provides the best possible code based on value probability [20].

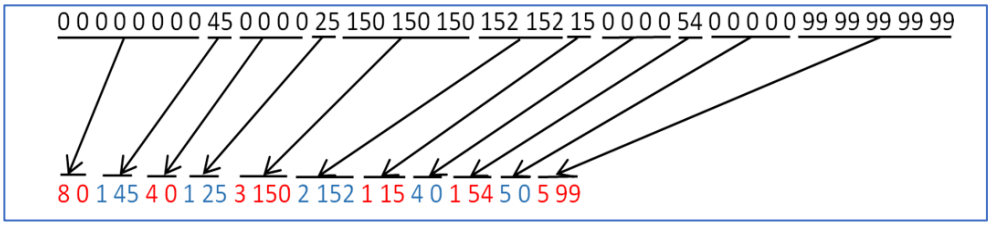

Figure 5: The RLE process converts the successively similar numbers into numbers that can be compressed due to their probabilities

3.3.2 Ignoring Trivial Values

Before applying RLE on long series, it was noticed that tiny values (1, 2, or 3), which mostly occur outside the fluid motion area, break the series of zeros as in Fig 6. It shows a real snapshot of the different results of two ROI images. Due to the high occurrence of zeros, values are obviously from outside fluid-motion areas; they can be ignored and converted to zeros to create a long continuous series of zeros. They can be ignored due to two justifications; firstly, they can occur from imaging errors[21]. Secondly, even if they form real differences, such tiny differences refer to insignificant changes, and the value level remains almost the same [22]. This paper ignores only tiny differences within a set of zeros, while other differences that occur within fluid-motion areas are kept to preserve fluid changes as they are. The maximum value of ignored differences is determined depending on the quality of the decompressed images. In other words, this work ignores only differences that do not affect the PSNR value of decompressed images.

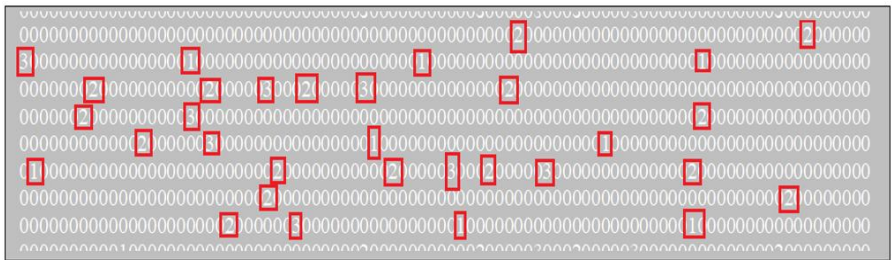

Figure 6: Real snapshot from difference results between two ROI images, where tiny values break the series of zeros

3.3.3 Doubling CR Performance

After accomplishing RLE and Huffman coding techniques, the result values are compressed using a new encoding fashion. Using the standard equation of contrast adjustment [23], result values are converted from the (0- 255) range into the (0- 15) range using Equation 2:

$$x_{new} = round\left[\frac{(x_{old} - min)}{(max - min)}\right] \times 15 \qquad \dots (2)$$

Where x_{old}: is the original compressed value after RLE and Huffman coding, min, max: are the minimum and maximum values, x_{new}: is the result value of the (0- 15) range.

Converting the values in the (0- 15) range requires only 4 bits instead of 8 bits to represent them. This means that each value can be concatenated into one byte, which leads to double the CR value yielded after applying RLE and Huffman coding. The next mathematical example illustrates the conversion process. In Table 1, the first row contains random numbers in the (0-255) range, and the second row contains their minimum and maximum values. After converting them into the (0-15) range, the third row contains these numbers.

Table 1 illustrates converting values from the (0- 255) range into the (0- 15) range.

(0-255) values	180	136	148	74	77	198	4	194	208	181	12	106	220	202
Min =4						**Max=200**								
(0- 15) values	12	9	10	5	5	13	0	13	14	12	1	7	15	14

To explain the proposed fashion of encoding, these numbers, shown in Table 1, are represented in binary digits as:

180=10110100; 136=10001000; 148=10010100; 74=01001010; 77=01001101; 198=11000110; 4=00000100; 194=11000010; 208=11010000; 181=10110101; 12=00001100; 106=01101010; 220=11011100; 202=11001010.

Due to the definition of bytes[24], each needs 8 bits to be represented. Conversely, (0- 15) range values need only 4 bits to be represented.

12= 1100& 9=1001; 10=1010; 5=0101; 5=0101; 13=1101; 0=0000; 14=1110; 12=1100; 1=0001; 7=0111; 15=1111; 14=1110

Each two successive numbers, of (0- 15) range, are concatenated into one byte as follows:

12= 1100& 9=1001 are concatenated into one 8-bit byte as 11001001=201 and so on for the remaining numbers. The number of result numbers will be 7 as follows instead of the 14 numbers used in this example:

201; 165; 93; 13; 236; 23; 254

As illustrated in Fig 7, the original size of 14 numbers results in the size of 7 numbers, which equals half of the original numbers, and the CR value is doubled due to the CR equation.

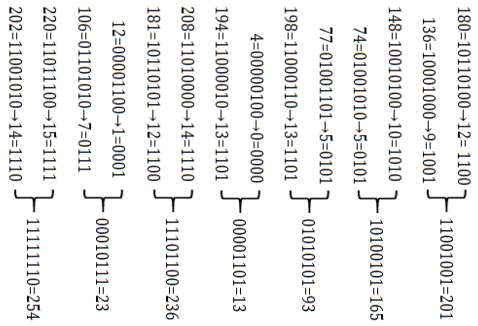

Figure 7: Doubling CR ratio by shrinking the number of values into the half-size

$$CR = \frac{Original\ data\ size}{Compressed\ data\ size} \quad \dots 3$$

$$CR_{new} = \frac{(Original\ data\ size)}{1/2 \times Compressed\ data\ size} \quad \dots 4$$

$$CR_{new} = 2 \times CR \quad \dots 5$$

Although Equation 2 in not a lossless retrieval, high yielded results of PSNR showed that the loss amount is trivial and retrieved data recorded significantly high effectiveness. Finally, the entire proposed compression scheme can be shown in Figure 5.

4. RESULTS AND DISCUSSION

The experiments of this work were designed to compress medical DVF images captured for the Pharynx and Esophagus. Different measures were applied to evaluate experimental results, such as cross-correlation (Equation 1), CR (Equation 3), and PSNR. To evaluate restored-images quality after applying different applications, the PSNR measure was proposed. In image compression, it's usually to evaluate the restored image after lossy and near-lossless compression. It depends on Mean Squared Error measures (Equation 5) that gauge the differences between original (O_{im}) and restored (Rim) images, which should be zero for lossless compression [25].

$$MSE = \frac{1}{M \times n} \sum_{i=1}^{N} \sum_{j=1}^{M} (O_{im} - R_{im})^2 \quad \dots 5$$

$$PSNR = 20log_{10}\left(\frac{MAX_O}{\sqrt{MSE}}\right) \quad \dots 6$$

Where MAXo: is the maximum pixel value in original images. The higher PSNR leads to a higher similarity between original and restored images, where in lossless compression, MSE=0, then PSNR=∞. Yet, yielding PSNR between 30 and 50 is acceptable in different literatures [26]. This paper combines RLE and Huffman coding, and it proposes applying RLE then Huffman due to the huge amount of sequential values (0's). Table 2 illustrates the best and average yielded PSNR values for applying different combinations between RLE and Huffman on 65 sets of DVF images.

Table 2: The best and averages of yielded values for PSNR yielded from combining RLE

	Best PSNR	**Average**
RLE then Huffman	58.79	51.98
Huffman then RLE	48.88	37.63

Subtracting sequential images with a first reference one has two ways, where the first one is to consider the reference in each subtraction process. In this way, the subtraction refers to the ideal patient case before treating it and its difference from each stage of treatment. Second, consider each successive difference to gauge the update changes. The second way yielded better CR values due to higher correlations between each stage and its successor than its correlation with the reference one. Table 3 shows a sample set of DVF images numbered from 0 (reference) to 9. The reference is not mentioned in both; image numbers start from 1.

In different images, sets of ignorable values indicate capturing errors or insignificant changes in pixel values. Most of these values vary between (1- 3), but still, there are other higher differences. As ignoring higher differences increases the yielded CR, the PSNR value decreases, indicating some distortion in the decompressed images. Ignoring more than 3 decreases yielded PSNR values. Fig 8 explains PSNR and CR values along with 1- 7. Ignoring more than 3 decreases the PSNR value against insignificant increments in CR values.

In contrast adjustment, an 8-bit byte is converted into 4-bit numbers to concatenate each two of them into one byte. This process decreases compressed-data size to half, which doubles compression performance in the form of CR values. Results showed that decreasing an 8-bit byte into less than 4-bit numbers decreases the yielded PSNR values and increases the compression scheme's complexity. On the other side, no significant increment was witnessed in CR values.

Table 3: CR and $r_{x,y}$ values for two subtraction ways

DVF Images	Successive Diff.		Reference Diff.	
	CR	$r_{x,y}$	***CR***	$r_{x,y}$
1.	39	0.94	39	0.94
2.	40	0.96	40	0.92
3.	41	0.97	38	0.88
4.	45	0.95	37	0.91
5.	47	0.95	36	0.87
6.	48	0.96	37	0.9
7.	48	0.95	36	0.91
8.	49	0.97	35	0.92
9.	50	0.97	36	0.91

As benchmarking with previously published articles, the proposed compression scheme yielded superior results, recording the best compression rate with a specific set DVF (54.31). As an average performance for all studied DVF image sets, this work recorded (50.52) with (51.98) db for PSNR. Table 4 summarizes the previously yielded results in medical image compression using near-lossless image compression only, where lossy and lossless compression techniques were ignored for face comparison.

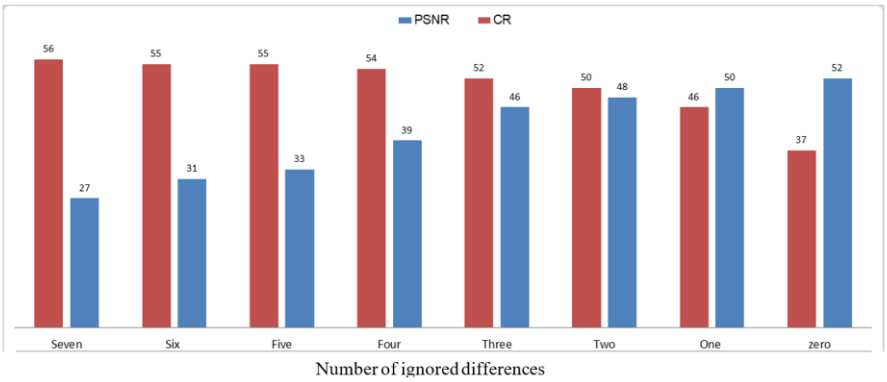

Figure 8: The number of ignored differences and their effects on CR& PSNR

5. CONCLUSION

This work focuses on processing a series of DICOM Video Fluoroscopy (DVF) images, divided into Regions of Interest (ROI) and non-ROI areas. Non-ROI areas containing no medical information are compressed using lossy methods to boost compression performance. In contrast, ROI areas are compressed with lossless techniques to preserve sensitive medical data. By subtracting sequential ROI images, we can highlight differences between successive images, turning similar areas with no fluid motion into zeros. This approach proves more effective than applying coding techniques to the images directly. After subtraction, we ignore trivial values that disrupt long sequences of zeros. These trivial values often represent minor differences or imaging errors, particularly in non-ROI areas. Zero areas are ideal for compression techniques that exploit a long series of similar values. Run-length encoding (RLE) works well for compressing these lengthy sequences of identical values. The compressed results from RLE are then processed with Huffman Coding, which improves compression efficiency and ratio. Sequential lossless coding techniques introduce a new strategy that doubles the Compression Ratio (CR). Applying RLE before Huffman Coding yields better results than the reverse order because RLE handles long sequences of zeros more effectively. Subtracting successive ROI images provides superior performance compared to subtracting each ROI image from a reference image, thanks to the high correlation between successive images, which generates more zeros. We manage the impact of ignoring trivial values by monitoring the Peak signal-to-noise ratio (PSNR) of the decompressed images, with ignored values ranging from 1 to 3. Our method has outperformed others, achieving a best CR value of 54.31 and a best PSNR value of 58.79

Table 4: Summarizes the benchmarking results with previously published works in near-lossless compression fields.

Method	CR	PSNR
Elhannachi, et al (2017)[27]	39.33	45.07
Gowda, et al (2022) [8]	49.1	38.13
Abdellatif, et al (2022) [9]	36.75	43.85
Bindu, & Afthab (2021) [10]	37.49	43.04
Proposed Scheme	**50.52**	**51.98**

CONFLICT OF INTEREST

The authors declare that there is *no conflict of interest* regarding the publication of this paper.

REFERENCES

[1] S. A. B. Aziz *et al.*, "A Performance Review for Hybrid Region of Interest-Based Medical Image Compression," *IEEE Access*, vol. 11, pp. 98025–98038, 2023, doi: 10.1109/ACCESS.2023.3312265.

[2] S. Jamil, M. J. Piran, M. U. Rahman, and O. J. Kwon, "Learning-driven lossy image compression: A comprehensive survey," *Eng. Appl. Artif. Intell.*, vol. 123, p. 106361, 2023, doi: 10.1016/j.engappai.2023.106361.

[3] M. A. Rahman, M. Hamada, and J. Shin, "The impact of state-of-the-art techniques for lossless still image compression," *Electron.*, vol. 10, no. 3, pp. 1–40, 2021, doi: 10.3390/electronics10030360.

[4] U. Singh and M. Kumar, "A Review: Compression on Medical Images," *A Rev. Compression Med. Images Artic. Int. J. Eng. Tech. Res.*, vol. 11, pp. 103–109, 2022, doi: 10.17577/IJERTV11IS040058.

[5] O. Keles, M. A. Yilmaz, A. M. Tekalp, C. Korkmaz, and Z. Dogan, "On the Computation of PSNR for a Set of Images or Video," in *2021 Picture Coding Symposium, PCS 2021 - Proceedings*, IEEE, 2021, pp. 1–5. doi: 10.1109/PCS50896.2021.9477470.

[6] D. Mishra, S. K. Singh, and R. K. Singh, "Deep Architectures for Image Compression: A Critical Review," *Signal Processing*, vol. 191, p. 108346, 2022, doi: 10.1016/j.sigpro.2021.108346.

[7] S. A. Aziz *et al.*, "A review on region of interest-based hybrid medical image compression algorithms," *Telkomnika (Telecommunication Comput. Electron. Control.*, vol. 18, no. 3, pp. 1650–1657, 2020, doi: 10.12928/TELKOMNIKA.v18i3.14900.

[8] D. Gowda V *et al.*, "A novel method of data compression using ROI for biomedical 2D images," *Meas. Sensors*, vol. 24, p. 100439, 2022, doi: 10.1016/j.measen.2022.100439.

[9] H. Abdellatif, T. E. Taha, R. El-Shanawany, O. Zahran, and F. E. Abd El-Samie, "Efficient ROI-based compression of mammography images," *Biomed. Signal Process. Control*, vol. 77, p. 103721, 2022, doi: 10.1016/j.bspc.2022.103721.

[10] P. V. Bindu and J. Afthab, "Region of Interest Based Medical Image Compression Using DCT and Capsule Autoencoder for Telemedicine Applications," in *2021 4th International Conference on Electrical, Computer and Communication Technologies, ICECCT 2021*, IEEE, 2021, pp. 1–7. doi: 10.1109/ICECCT52121.2021.9616748.

[11] E. Gingold, "Modern Fluoroscopy Imaging Systems," *Radiat. Saf. Adult Med. Imaging*, pp. 1–9, 2014, [Online]. Available: http://www.imagewisely.org/imaging-modalities/fluoroscopy/articles/gingold-modern-systems

[12] B. Pervan, S. Tomic, H. Ivandic, and J. Knezovic, "MIDOM—A DICOM-Based Medical Image Communication System," *Appl. Sci.*, vol. 13, no. 10, p. 6075, 2023, doi: 10.3390/app13106075.

[13] J. Sra *et al.*, "Computed tomography-fluoroscopy image integration-guided catheter ablation of atrial fibrillation," *J. Cardiovasc. Electrophysiol.*, vol. 18, no. 4, pp. 409–414, 2007, doi: 10.1111/j.1540-8167.

[14] J. P. Miller, C. R. Pennypacker, and G. L. White, "Optimal Image Subtraction Method: Summary Derivations, Applications, and Publicly Shared Application Using IDL," *Publ. Astron. Soc. Pacific*, vol. 120, no. 866, pp. 449–464, 2008, doi: 10.1086/588258.

[15] R. A. Bahri, S. Maleki, A. Shafiee, and P. Shobeiri, "Ultrasound versus fluoroscopy as imaging guidance for percutaneous nephrolithotomy: A systematic review and meta-analysis," *PLoS One*, vol. 18, no. 3 March, p. e0276708, 2023, doi: 10.1371/journal.pone.0276708.

[16] T. V Vorburger *et al.*, "Applications of cross-correlation functions," *Wear*, vol. 271, no. 3–4, pp. 529–533, 2011, doi: 10.1016/j.wear.2010.03.030.

[17] A. A. Hussain, G. K. Al-Khafaji, and M. M. Siddeq, "Developed JPEG Algorithm Applied in Image Compression," in *IOP Conference Series: Materials Science and Engineering*, IOP Publishing, 2020, p. 32006. doi: 10.1088/1757-899X/928/3/032006.

[18] C. Reich, B. Debnath, D. Patel, and S. Chakradhar, "Differentiable jpeg: The devil is in the details," in *Proceedings of the IEEE/CVF Winter Conference on Applications of Computer Vision*, 2024, pp. 4126–4135. doi: 10.1016/j.asoc.2020.106114.

[19] N. A. Khairi and A. B. Jambek, "Run-Length Encoding (RLE) Data Compression Algorithm Performance Analysis on Climate Datasets for Internet of Things (IoT) Application," *Int. J. Nanoelectron. Mater.*, vol. 14, no. Special Issue InCAPE, pp. 191–197, 2021, doi: 10.1109/ICECCT52121.2021.9616748.

[20] A. Varshney, K. Suneetha, and D. K. Yadav, "Analyzing the Performance of Different Compactor Techniques in Data Compression & Source Coding," in *2024 International Conference on Optimization Computing and Wireless Communication, ICOCWC 2024*, IEEE, 2024, pp. 1–6. doi: 10.1109/ICOCWC60930.2024.10470923.

[21] J. N. Itri, R. R. Tappouni, R. O. McEachern, A. J. Pesch, and S. H. Patel, "Fundamentals of diagnostic error in imaging," *Radiographics*, vol. 38, no. 6, pp. 1845–1865, 2018, doi: 10.1148/rg.2018180021.

[22] W. Burger and M. J. Burge, Digital Image Processing. 2022. doi: 10.1007/978-3-031-05744-1.

[23] B. S. Rao, "Dynamic Histogram Equalization for contrast enhancement for digital images," *Appl. Soft Comput. J.*, vol. 89, p. 106114, 2020, doi: 10.1016/j.asoc.2020.106114.

[24] A. Radonjic and V. Vujicic, "Integer Codes Correcting Single Errors and Random Asymmetric Errors within a Byte," *J. Syst. Sci. Complex.*, vol. 33, no. 6, pp. 2103–2113, 2020, doi: 10.1007/s11424-020-8145-9.

[25] A. M. John, K. Khanna, R. R. Prasad, and L. G. Pillai, "A review on application of fourier transform in image restoration," in *Proceedings of the 4th International Conference on IoT in Social, Mobile, Analytics and Cloud, ISMAC 2020*, IEEE, 2020, pp. 389–397. doi: 10.1109/I-SMAC49090.2020.9243510.

[26] S. Jamil, M. J. Piran, M. U. Rahman, and O. J. Kwon, "Learning-driven lossy image compression: A comprehensive survey," *Eng. Appl. Artif. Intell.*, vol. 123, 2023, doi: 10.1016/j.engappai.2023.106361.

[27] S. A. Elhannachi, N. Benamrane, and T. A. Abdelmalik, "Adaptive medical image compression based on lossy and lossless embedded zerotree methods," *J. Inf. Process. Syst.*, vol. 13, no. 1, pp. 40–56, 2017, doi: 10.3745/JIPS.02.0052.